SSRG International Journal of Electrical and Electronics Engineering
ISSN: 2348-8379/ https://doi.org/10.14445/23488379/IJEEE-V11I11P113

Volume 11 Issue 11, 122-130, November 2024

Original Article

Electrical Characteristics of Plasma Jet Depending on Operating Voltage Amplitude at Industrial Frequency

Hoa Thi Truong[1], Van Nhan Truong[2]

[1,2]*The University of Danang - University of Technology and Education, 48 Cao Thang, Danang, Vietnam.*

[1]*Corresponding Author : tthoa@ute.udn.vn*

Received: 08 September 2024 Revised: 09 October 2024 Accepted: 07 November 2024 Published: 30 November 2024

Abstract *- This study investigates the electrical characteristics of Dielectric Barrier Discharge (DBD)-based Atmospheric Pressure Plasma Jets (APPJs) with varying input voltage amplitudes at industrial frequencies. The experiments show that increasing voltage amplitude significantly enhances discharge pulse density driven by a spatial electric field formed on the dielectric layer during each half-cycle and lowers the breakdown threshold of discharge onset. Increasing the voltage amplitude results in a higher density of discharge pulses, enhancing the plasma's reactive output. This increase in discharge pulse density is accompanied by a reduction in the breakdown threshold, making it easier to initiate and sustain plasma discharges at higher voltages. The study also reveals that under the experimental condition, energy consumption by discharge increases linearly with voltage amplitude up to 3 kV, independent of gas flow rate. Beyond 3 kV, energy consumption depends on gas flow, with higher rates leading to greater energy usage. These findings offer critical insights into DBD plasma jet behavior, highlighting the importance of voltage amplitude and gas dynamics in optimizing APPJ performance, particularly in industrial power source applications.*

Keywords *- Atmospheric pressure plasma jet, Non-thermal plasma, Dielectric barrier discharge, Plasma application, Plasma characteristics.*

1. Introduction

Currently, Atmospheric Pressure Plasma Jets (APPJs) have garnered significant attention because of their diverse applications, as well as their near-field functioning at ambient temperature without vacuum and inexpensive production costs. Because it can operate at near room temperature without a vacuum, the DBD-based APPJ devices are compact and portable.

Due to their simple design and operation, APPJ devices are cost-effective compared to other plasma technologies, especially in large-scale and continuous processing. APPJ is versatile and suitable for on-site treatments in various settings, including in medicine for wound healing and cancer treatment, as well as for modifying surface properties in materials science in environmental science for pollutant degradation and air purification and for sterilization and decontamination in the healthcare and food industries [1, 2].

In practice, plasma jets can be generated in various configurations and designs. However, a common configuration is based on the Dielectric Barrier Discharge (DBD) principle in biological, environmental, and medical applications. DBD-based APPJ offers several advantages in various applications due to its unique properties and capabilities; DBD-based APPJ can generate a stable and focused plasma stream to open air with high concentrations of reactive species, including charged particles, metastable species, highly reactive radicals and UV radiation [3, 4].

The basic configuration of an APPJ consists of a high-voltage connecting electrode and a ground electrode encircling a dielectric layer, which can be a quartz or glass tube. The creation of electrical discharge is easier and more developed in systems with floating electrodes. This form of plasma is created using a variety of power sources, including Direct Current (DC), high-voltage Alternating Current (AC), Microwaves (MW), Radio Frequency (RF), and pulsed DC power sources [5-8].

In a DBD-based APPJ configuration, dielectric layer voltage, frequency, and properties significantly influence discharge behavior [6, 9]. Charges accumulated on the surface of dielectric layers create a memory effect, causing discharges to either tend to reignite at previous locations in bi-polar high-frequency mode or distribute across the electrode surface in high-voltage uni-polar pulse mode [10, 11].

The power sources used in generating Atmospheric Pressure Plasma Jets (APPJs) play an important role in influencing the characteristics of the APPJs. It affects not only the shape and stability of the plasma but also other important parameters such as temperature, electron density, and the chemical reactions occurring within the plasma. The APPJ operating with the DBD principle is often generated by pulsed power supplies or high-voltage AC power sources, particularly at frequencies in the range of 10 to 100 kHz [1, 2, 12]. This type of power source helps prevent the formation of high-temperature arcs, creating stable plasma suitable for surface treatment and biomedical applications. Increasing input power generally leads to an increase in plasma density and electron temperature [13, 14]. However, too much power can cause unstable arc formation, reducing plasma efficiency [15].

Additionally, the frequency of the power source significantly affects plasma characteristics. High frequencies typically produce plasma with higher electron density and stronger chemical reactions, while lower frequencies generally create more stable and easier-to-control plasma [16]. Higher voltages usually result in stronger ionization, creating a plasma with higher density. However, excessively high voltages can cause instability in the plasma. Power sources with square, triangular, or sinusoidal pulses can affect the energy distribution within the plasma, thereby influencing chemical reactions and energy conversion processes [8]. These factors indicate that selecting the appropriate power source is extremely important for adjusting APPJ characteristics to fulfill the unique needs of each application [20]. Understanding the impact of the power source helps researchers and engineers optimize plasma operating conditions, thereby improving efficiency and expanding the potential applications of APPJ in industry and biomedicine [17, 18, 19, 21].

In most prior research, plasma jets are typically produced using high-voltage sources or high-frequency pulse sources, which tend to be costly. Consequently, this study employs high-voltage power sources at an industrial frequency to make plasma jet applications more accessible. While many studies have focused on high-frequency, high-voltage sources, there is still a lack of detailed research on the effects of low-frequency power sources. Memory effect in the DBD principle can influence the discharge behaviour by retaining residual charges on the dielectric surface from previous cycles, especially under low-frequency operation. This effect can distort the electric field in subsequent discharge cycles, leading to irregular plasma formation and potentially affecting the uniformity and stability of the discharge process. In this study, an APPJ in Ar gas was generated by a sinusoidal voltage source at industrial frequency. The electric processes and characteristics, in turn, with increasing amplitude of applied discharge voltage, were inspected by measuring the voltage and current waveforms. The effects of applied voltage amplitude were investigated and identified from the experimental results, and then the discharge mechanism of the plasma jet system operating at industrial frequency was analyzed.

2. Experimental Setup and Conditions

The experimental setup for generating APPJ is shown in Figure 1. The apparatus is arranged in four main parts: gas feeding system, power supply, plasma jet reactor, and experimental data acquisition system. Argon gas used for plasma generation was fed into the discharge zone from the top of the tube and then exhausted into the open air at the bottom tip. The flow rate ranged from 1 to 5 slm. A high-voltage power system is a sinusoidal high-voltage source operating at the low frequency of 50 Hz, including a primary power supply and a step-up transformer. The primary power supply is a commercial adjustable AC power source with an amplitude of input voltage that can change smoothly from 0 to 230 V. A step-up transformer boosts the output of the primary power supply and is then connected to the high voltage electrode of the discharge tube via a 5 MΩ resistor. The 5 MΩ resistor is used to limit current and supply from the source to ensure stable operation of the experimental system. In this arrangement, the amplitude of the applied voltage on the High Voltage (HV) electrode was changed in a range of 1 to 4 kV.

The structure of the APPJ reactor is illustrated in Figure 2. The plasma jet reactor comprises an HV electrode placed inside a coaxial tube and a grounded electrode in the form of a copper wire wound in a helical pattern around the outer tube's surface. The tubes are made from quartz and play the role of dielectric layers in this configuration. The HV electrode is a 100 mm long tungsten needle with 1 mm diameter. The tube has dimensions of 8.5 mm outer diameter, 6.5 mm inner diameter, and 110 mm in length. The tip of the HV electrode is positioned 10 mm away from the end of the tube.

The data acquisition system includes an oscilloscope connected to high-voltage and current probes. The voltage at the powered electrode was measured using a high voltage probe (Tektronix P6015A). The discharge current was monitored using a 10 Ω shunt resistor (BPC10100J) connected in series between the grounded electrode and the ground point. The discharge current was determined by measuring the voltage drop across the shunt resistor and dividing the voltage value by the resistance of 10 Ω of the shunt resistor. The shunt resistor is typically made from manganin, a highly precise and non-inductive material with a low resistance value. Its function is to reduce voltage by creating an alternative path with very little resistance. Therefore, it allows accurate, current measurement without affecting the main circuit while limiting harmonic currents caused by parasitic capacitances and conductors.

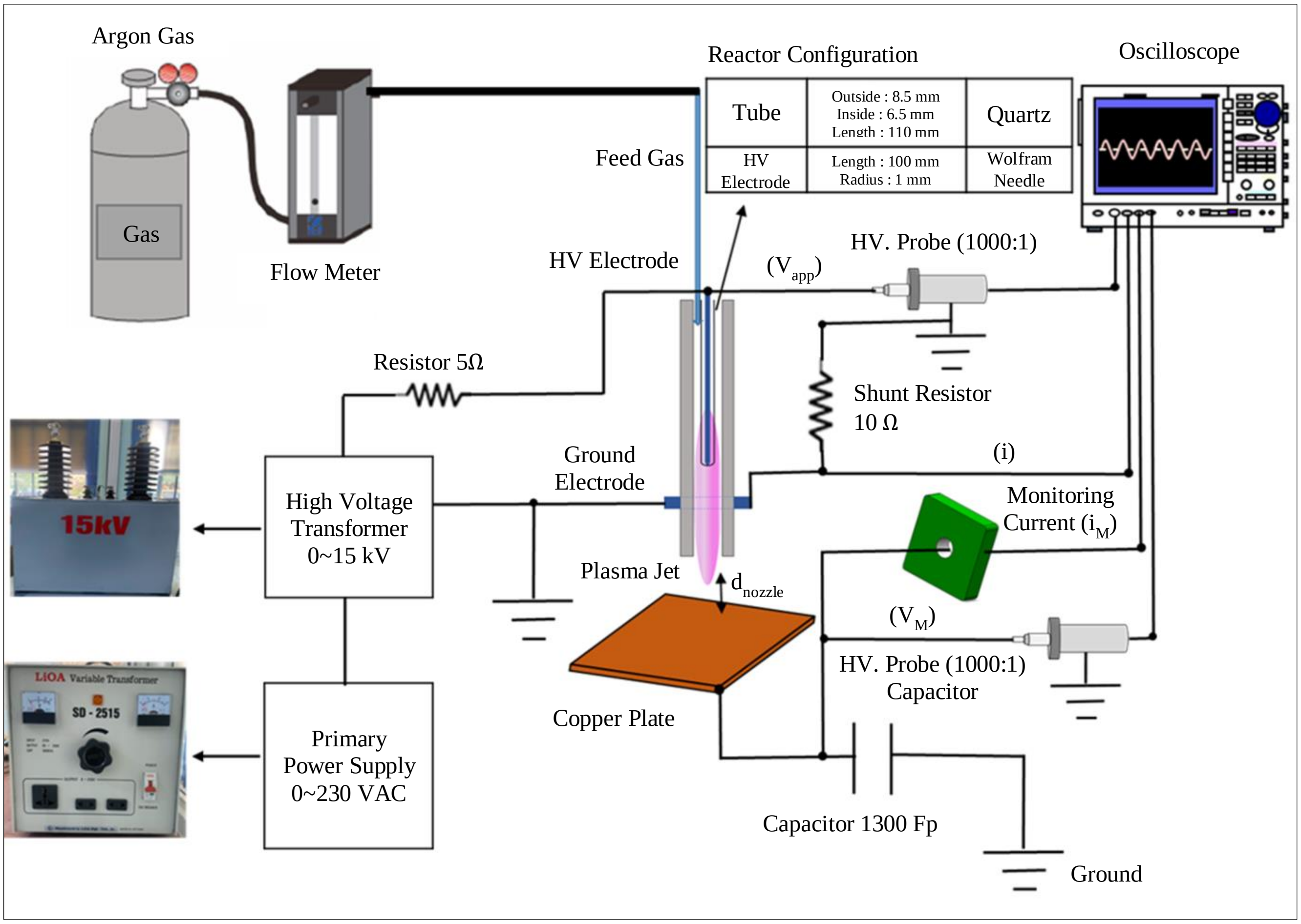

Fig. 1 Experimental setup

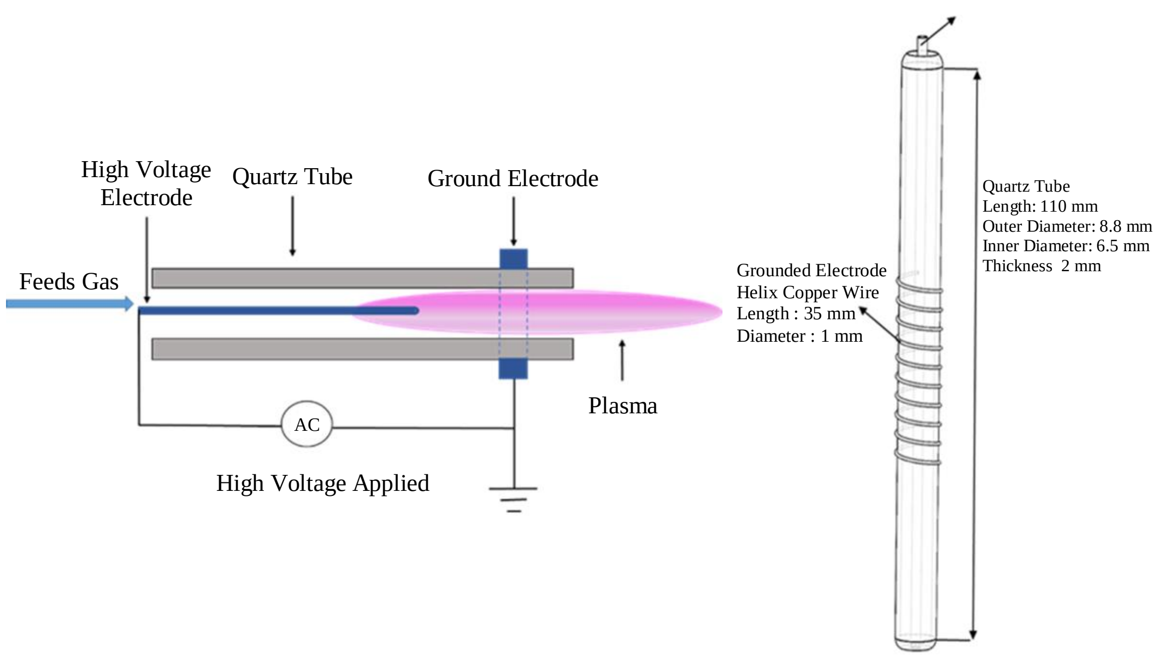

(a) **(b)**

Fig. 2 The configuration of DBD based-plasma jet (a) Configuration, and (b) Nozzle structure.

Table 1. Experimental condition

Primary Power Supply	0 ~ 230 VAC
High Voltage Transformer	0 ~ 15 kV
Frequency	50 Hz
Working Gas	Argon (1÷5 slm)
Temperature	Room Temperature
Pressure	Atmospheric Pressure

The power consumption can be estimated by analyzing the Q–V Lissajous figure. The Q–V Lissajous figure was obtained by placing a copper plate as an interactive object to collect charge particles transferred by the discharge and accumulating on the dielectric layer. A monitoring capacitor (C_M) with a capacitance of 1300 pF is connected in series with the copper plate to measure the amount of charge accumulated on the dielectric layer after each discharge cycle.

Similarly, a voltage probe (Tektronix P6015A) measured the voltage drop on the monitoring capacitor. The data has been recorded by digital oscilloscopes (Tektronix TBS 1102B-EDU-100 MHz- 2.5G S/s and Tektronix MDO3022-200 MHz-2.5G S/s). Experiments have been conducted with a condition presented in Table 1.

3. Results and Discussion

Firstly, the experiment sought to investigate the impact of increasing the amplitude of the industrial voltage source on the discharge process. The applied voltage amplitude was adjusted from 1 to 4 kV in 0.5 kV increments, using Ar gas at a flow rate of 3 slm. The experimental results are presented in Figure 3, which displays the waveforms of the applied voltage (V_{app}), discharge current (I), and voltage drop across the monitor capacitor (V_M). The appearance of current pulses can detect discharge occurrence.

As seen in Figure 3, at the voltage amplitude of 1 kV, no discharge occurs. However, when the voltage amplitude is increased beyond 1.5 kV, the appearance of current pulses indicates that the discharge has ignited. As the amplitude of applied voltage increased, the breakdown threshold required to initiate discharge decreased significantly, leading to an earlier onset of discharge, an increase in discharge frequency, and a greater number of discharge pulses per cycle.

Additionally, the discharge becomes particularly dense at both the rising and falling edges of the sinusoidal voltage waveforms just before reaching the peaks for applied voltage amplitudes ranging from 2 to 4 kV. The number of discharge current pulses per cycle and the breakdown voltage threshold (the instantaneous value of the voltage at which discharge begins for each voltage amplitude) were estimated. Figure 4 collectively illustrates the behavior of the APPJ as the applied voltage amplitude increases.

Discharge pulses were counted using a data processing method only when the minimum current pulse threshold was 4 mA or higher, which ensured that interferences were ignored. In Figure 4(a), the graph illustrates the relationship between the increased applied voltage amplitude and the number of discharge current pulses per cycle. In contrast, Figure 4 (b) shows the effect of the increase in applied voltage amplitude on the breakdown threshold of the temporary voltage value at which the discharge initiates.

The breakdown threshold of the temporary voltage value has been calibrated by the value at which the first discharge current peak appeared in each haft cycle of the applied voltage waveform, denoted as (V_B), as shown in Figure 3. The experiment was conducted at three different flow rates of 1, 3, and 5 slm, maintaining a laminar flow of the working gas to ensure reproducibility [21].

The experiments showed that increasing the input voltage increases the density of discharge pulses. The data clearly demonstrate that the number of discharge pulses increases quasi-exponentially with the increased applied voltage amplitude. At the same time, the breakdown voltage threshold decreases similarly, dropping from an initial instantaneous value of the voltage of 2 kV to zero, meaning that the discharge initiates at a lower temporary voltage value as the applied voltage amplitude becomes higher.

The experimental results for the DBD-based Atmospheric Pressure Plasma Jet (APPJ) can be interpreted by examining the behavior of the dielectric layer during the discharge process. Specifically, during each discharge pulse, especially at the positive voltage's half-cycle, charges accumulate on the dielectric layer's surface. This charge accumulation forms a spatial electric field within the discharge tube. As the voltage from the source reverses during the negative half-cycle, this spatial electric field aligns in the opposite direction to the original electric field provided by the source. Nonetheless, when the source voltage returns to the positive half-cycle, the spatial electric field's direction becomes again aligned with the source voltage.

The presence of a spatial electric field generated by stored charges on dielectric layers inside the discharge tube enhances the total electric field, augmenting the electric field originated by the source. This enhancement results in the discharge occurring at a lower voltage, leading to a higher density of discharge pulses as the input voltage increases. Furthermore, an increase in the amplitude of the applied voltage leads to a faster rate of voltage rise, contributing to the intensification of the discharge process.

Even if the electric field becomes saturated during discharge, the rise in voltage amplitude can cause the electric field at locations where discharge has already occurred to intensify further, triggering additional discharges. These discharges are further stimulated by surface electrons released from previous discharges or by free electrons already present in the discharge environment. Furthermore, as the voltage amplitude increases, the discharge spreads across the dielectric surface to areas and points that had not previously experienced discharge. This expansion of the discharge area results in a greater number of discharge pulses, which continues to increase until the applied voltage reaches its peak value. However, once the applied voltage reaches its peak and begins to decrease, there is no discharge during the downward slope of the voltage cycle. The discharge only resumes in the next half-cycle when the voltage increases again.

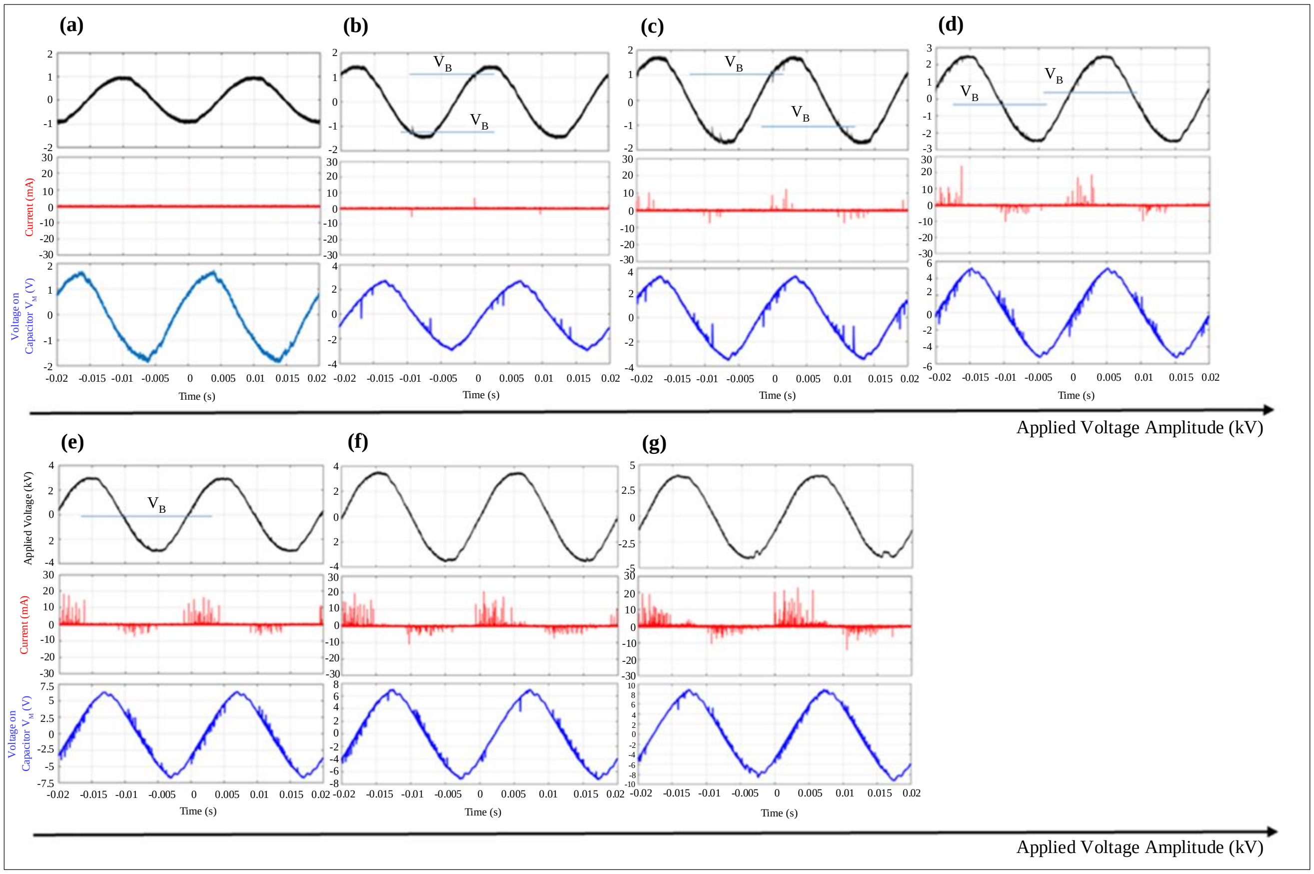

Fig. 3 Voltage, discharge current waveforms, and waveforms of voltage on monitor capacitor (V_M) measured at different applied voltage amplitudes (a) 1 kV, (b) 1.5 kV, (c) 2 kV, (d) 2.5 kV, (e) 3 kV, (f) 3.5 kV, and (g) 4 kV; in the figure V_B-denotes the breakdown voltage threshold.

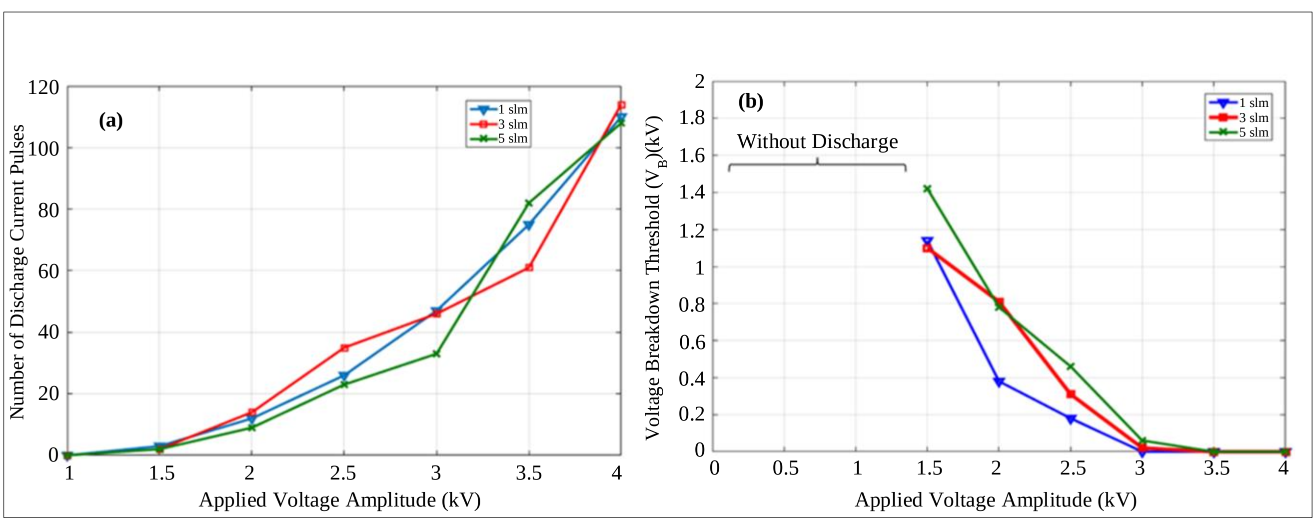

Fig. 4 Effect of increase in applied voltage amplitude on (a) Number of discharge current pluses, and (b) Breakdown voltage threshold.

The experimental results suggest that the discharge stops as the voltage drops from its peak until the voltage rises again in the following half-cycle. It is important to note that these effects may become less pronounced and more challenging to observe at high frequencies. At high-frequency operation, the time available for charge accumulation on the dielectric surface and the formation of the spatial electric field is reduced. This reduction may diminish the spatial electric field's impact on the discharge tube's overall electric field.

The findings align with the principles discussed, which emphasize the role of voltage amplitude and dielectric surface properties in controlling the distribution and reactivation of discharges. The study highlights that at low frequencies, as used in industrial applications, the interaction between the applied voltage and the dielectric surface leads to complex discharge patterns that can be optimized for specific applications by carefully managing the voltage amplitude and the timing of the applied pulses. The influence of applied voltage amplitude on the electrical characteristics of the APPJ has been examined using the Lissajous graph. To determine the power dissipated in the discharge, the area enclosed by the hysteresis loop of the Q-V diagram, known as the Lissajous figure, is calculated.

In a DBD system, the charge on the dielectric changes as the applied voltage varies during the AC cycle, forming a loop. The area of this Q-V hysteresis loop is directly related to the energy dissipated during each AC cycle. The average active power dissipated in the plasma discharge can be calculated using Equation (1) [22].

$$\overline{P_{DBD}} = \frac{1}{T}\oint_{\substack{one\\cycle}} V_{DBD}\, dQ_M = f \cdot S \qquad (1)$$

Where, T is the period, f is the frequency of power supply, and S is the area of the closed loop in the Lissajous graph.

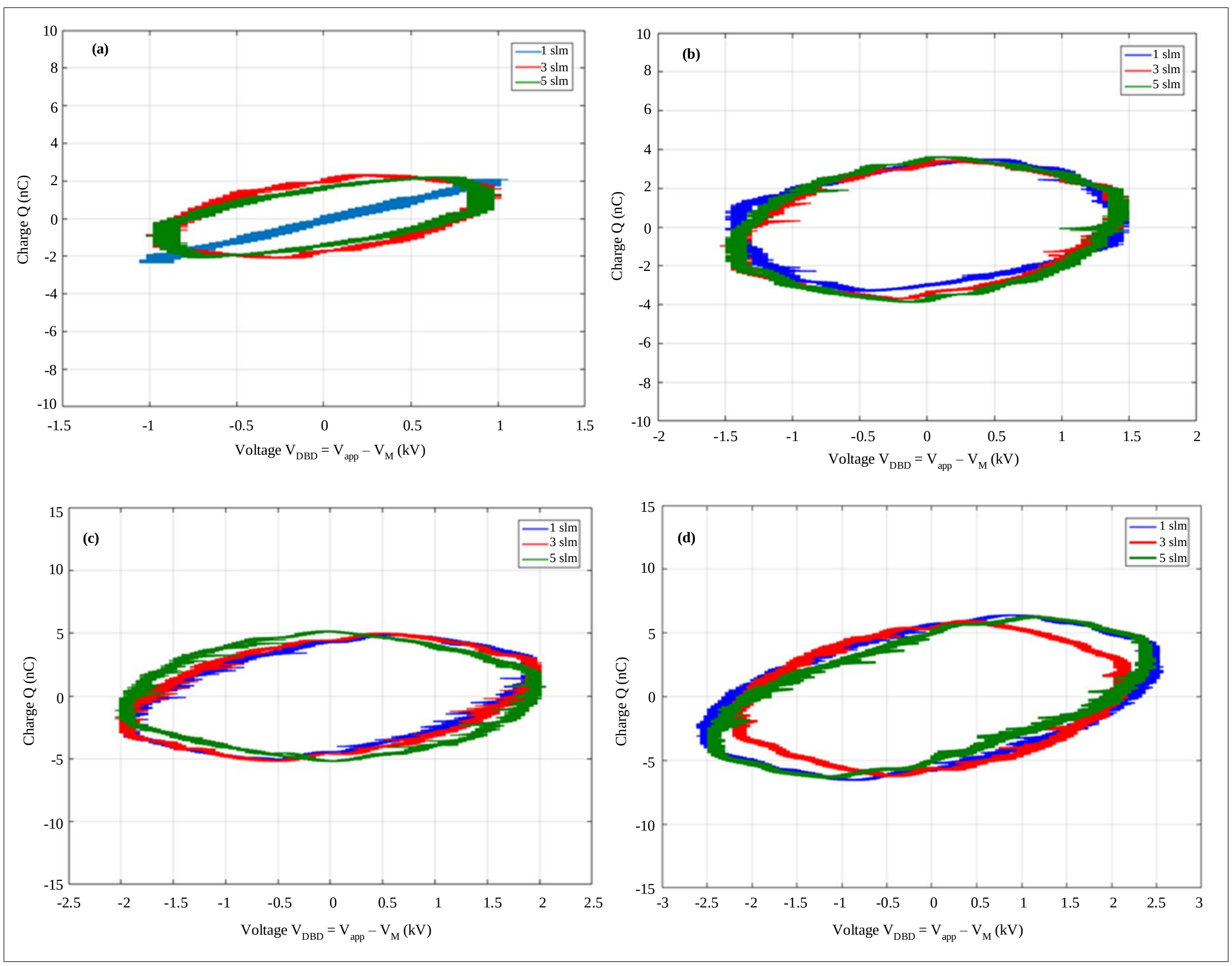

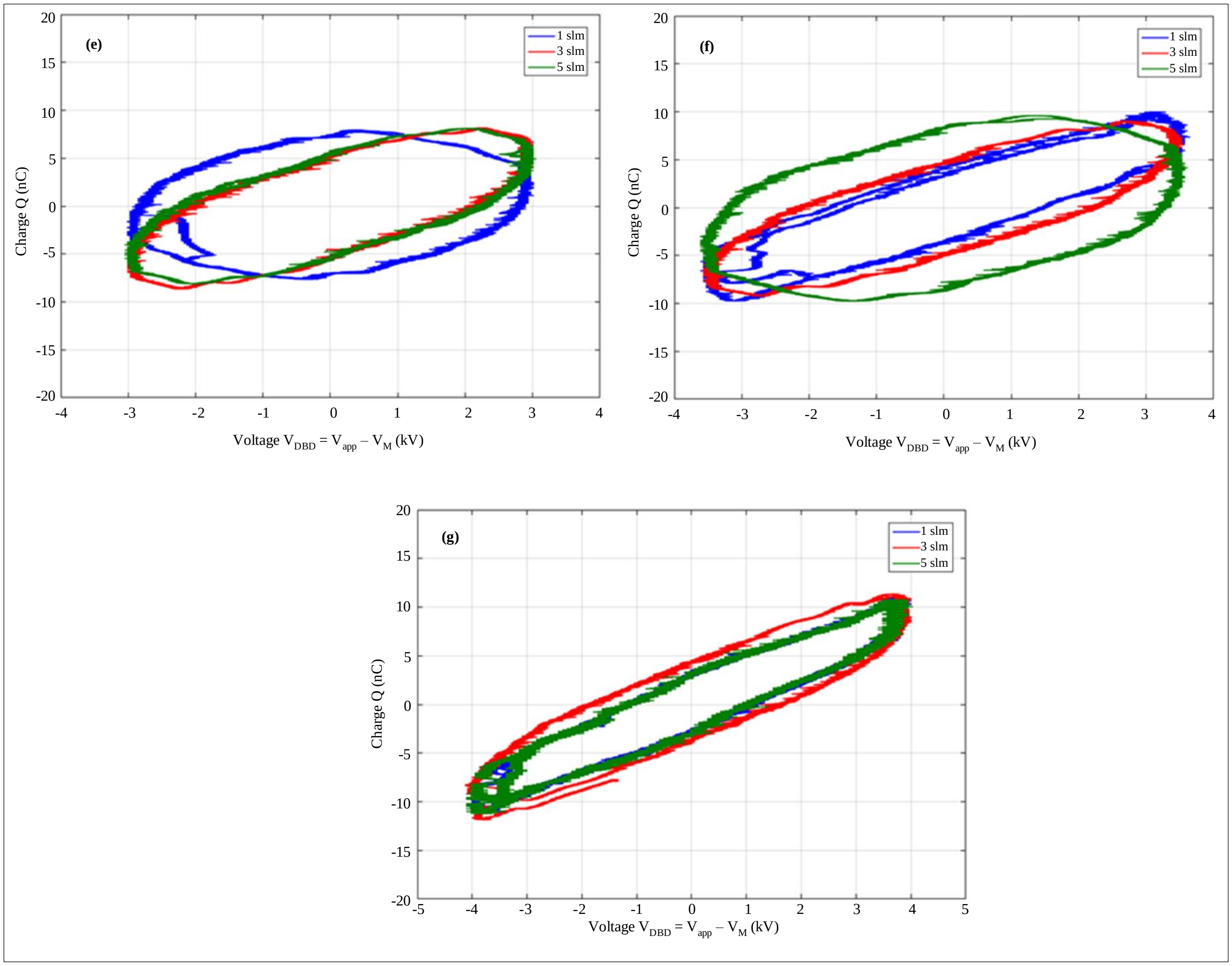

Fig. 5 Lissajous (Q-V) graphs with different applied voltage amplitudes (a) 1 kV, (b) 1.5 kV, (c) 2 kV, (d) 2.5 kV, (e) 3 kV, (f) 3.5 kV, and (g) 4 kV.

In Equation (1), the voltage across DBD-based APPJ can is calculated as,

$$V_{\mathrm{DBD}} = V_{\mathrm{app}} - V_{\mathrm{M}} , \quad (2)$$

and the charge on the monitor capacitor is calculated as,

$$Q_{\mathrm{M}}(t) = C_{\mathrm{M}} \cdot V_{\mathrm{DBD}}(t). \quad (3)$$

The Q-V loops for different applied voltage amplitudes under different gas flow rates 1, 3, and 5 slm are illustrated in Figure 5. The relationship between the input voltage amplitude and the energy consumed by the discharge in a DBD-based (APPJ) is illustrated in Figure 6. It can be seen that, with an increase in voltage amplitude from 0 to 3 kV, the energy consumed by the discharge increases linearly with the voltage. This trend is independent of the gas flow rate despite the applied voltage amplitude for discharge initiation being around 1.5 kV. This linear increase in energy consumption up to 3 kV suggests that the discharge process is primarily governed by the applied electric field, which consistently drives the plasma generation without significant interference from other factors, such as gas dynamics.

The independence from the gas flow rate during this phase indicates that the ionization and discharge mechanisms are stable and uniformly influenced by the increasing voltage alone. However, when the voltage amplitude exceeds 3 kV, the energy consumption by the DBD shows a clear dependence on the gas flow rate. At higher flow rates, the energy consumed by the discharges is significantly greater.

This phenomenon can be explained by the increased availability of fresh gas molecules at higher flow rates, which provides more material for ionization and subsequent discharge. The increased turbulence and movement of gas also contribute to more complex interactions between the electric field and the gas, enhancing the plasma's density and activity.

As a result, more energy is required to sustain the discharge at these elevated flow rates and higher voltage amplitudes.

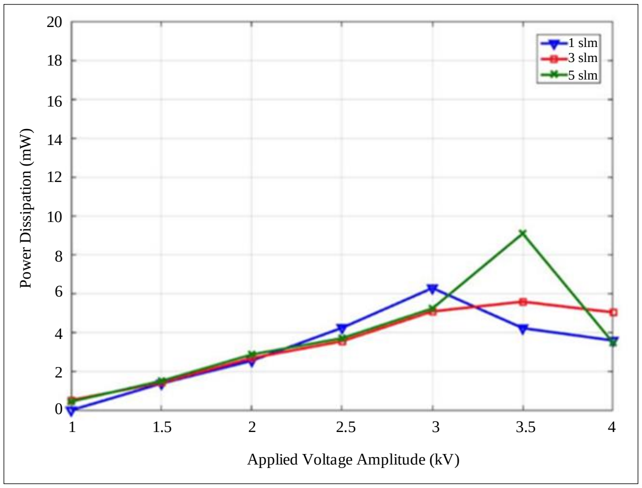

Fig. 6 Effect of the increase in applied voltage amplitude on the power dissipation of the discharge

The study suggests that at this low-frequency operation, similar to those used in industrial settings, raising the working voltage amplitude is a viable method to improve the performance of DBD-based APPJs. Moreover, the operating conditions, including gas flow rate and environmental factors, must be carefully managed. Higher voltage amplitudes can alter the plasma characteristics, potentially leading to more intense and localized discharges, which may impact the uniformity and stability of the plasma jet. It is also important to consider the implications of higher voltage levels on safety, energy efficiency, and overall system reliability.

4. Conclusion

This research revealed the electrical characteristics of DBD-based APPJs under different input voltage amplitudes. An increase in the voltage amplitude has led to a higher discharge pulse density and lowered the breakdown threshold for discharge onset during the half-cycle of the applied voltage cycle. Under the experimental condition, energy consumption increased linearly with voltage amplitude up to 3 kV regardless of the gas flow rate; however, beyond 3 kV, it started to depend on the gas flow rate. These findings highlighted the significance of voltage amplitude and gas flow dynamics in optimizing APPJ performance for applications, particularly in medical and environmental applications. By optimizing APPJ performance through a better understanding of electrical characteristics, the research offers pathways for improved treatment efficacy and efficiency.

The studies indicated that at low frequencies, corresponding to industrial frequencies, increasing the working voltage amplitude may be an effective option to enhance the performance of DBD-based APPJs. However, this approach requires careful consideration of the system configuration, electrical durability, and operating conditions related to the increased voltage levels.

References

[1] Mounir Laroussi et al., "Low-Temperature Plasma for Biology, Hygiene, and Medicine: Perspective and Roadmap," *IEEE Transactions on Radiation and Plasma Medical Sciences*, vol. 6, no. 2, pp. 127-157, 2022. [CrossRef] [Google Scholar] [Publisher Link]

[2] J. Winter, R. Brandenburg, and K.D. Weltmann, "Atmospheric Pressure Plasma Jets: An Overview of Devices and New Directions," *Plasma Sources Science and Technology*, vol. 24, 2015. [CrossRef] [Google Scholar] [Publisher Link]

[3] G. Divya Deepak et al., "A Low Power Miniaturized Dielectric Barrier Discharge Based Atmospheric Pressure Plasma Jet," *Review of Scientific Instruments*, vol. 88, 2017. [CrossRef] [Google Scholar] [Publisher Link]

[4] Ulrich Kogelschatz, "Dielectric-Barrier Discharges: Their History, Discharge Physics, and Industrial Applications," *Plasma Chemistry and Plasma Processing*, vol. 23, pp. 1-46, 2003. [CrossRef] [Google Scholar] [Publisher Link]

[5] Stephan Reuter, Thomas von Woedtke, and Klaus-Dieter Weltmann, "The kINPen- A Review on Physics and Chemistry of the Atmospheric Pressure Plasma Jet and Its Applications," *Journal of Physics D: Applied Physics*, vol. 51, 2018. [CrossRef] [Google Scholar] [Publisher Link]

[6] Xuechen Li et al., "Characteristics of an Atmospheric-Pressure Argon Plasma Jet Excited by a DC Voltage," *Plasma Sources Science and Technology*, vol. 22, 2013. [CrossRef] [Google Scholar] [Publisher Link]

[7] S. Hofmann et al., "Power Dissipation, Gas Temperatures and Electron Densities of Cold Atmospheric Pressure Helium and Argon RF Plasma Jets," *Plasma Sources Science and Technology*, vol. 20, no. 6, 2011. [CrossRef] [Google Scholar] [Publisher Link]

[8] Asma Begum et al., "Helium Plasma Jet Interaction with Different Target Materials and the Plasma Characteristics on the Irradiation Area," *European Physical Journal Applied Physics*, vol. 98, 2023. [CrossRef] [Google Scholar] [Publisher Link]

[9] G. Divya Deepak et al., "Electrical Characterization of Argon and Nitrogen Based Cold Plasma Jet," *European Physical Journal Applied Physics*, vol. 83, 2018. [CrossRef] [Google Scholar] [Publisher Link]

[10] Yong-Jie Zhou et al., "Nonequilibrium Atmospheric Pressure Plasma Jet Using A Combination of 50 kHz/2 MHz Dual-Frequency Power Sources," *Physics of Plasmas*, vol. 20, 2013. [CrossRef] [Google Scholar] [Publisher Link]

[11] Duc Ba Nguyen, Young Sun Mok, and Won Gyu Lee, "Enhanced Atmospheric Pressure Plasma Jet Performance by An Alternative Dielectric Barrier Discharge Configuration," *IEEE Transactions on Plasma Science*, vol. 47, no. 11, pp. 4795-4801, 2019. [CrossRef] [Google Scholar] [Publisher Link]

[12] Zhi Fang et al., "Discharge Processes and an Electrical Model of Atmospheric Pressure Plasma Jets in Argon," *The European Physical Journal D*, vol. 70, 2016. [CrossRef] [Google Scholar] [Publisher Link]

[13] Min Jeong Seong et al., "Effects of Operational Parameters on Plasma Characteristics and Liquid Treatment of a DBD-Based Unipolar Microsecond-Pulsed Helium Atmospheric Pressure Plasma Jet," *Physics of Plasmas*, vol. 30, 2023. [CrossRef] [Google Scholar] [Publisher Link]

[14] Bhagirath Ghimire et al, "Enhancement of Hydrogen Peroxide Production from an Atmospheric Pressure Argon Plasma Jet and Implications to the Antibacterial Activity of Plasma Activated Water," *Plasma Sources Science and Technology*, vol. 30, no. 3, 2021. [CrossRef] [Google Scholar] [Publisher Link]

[15] Yue Liu et al, "Micro Atmospheric Pressure Plasma Jets Excited in He/O_2 by Voltage Waveform Tailoring: A Study Based on a Numerical Hybrid Model and Experiments," *Plasma Sources Science and Technology*, vol. 30, no. 6 2021. [CrossRef] [Google Scholar] [Publisher Link]

[16] Benjamin Harris et al., "Ozone Production by An $He+O_2$ Radio-Frequency Atmospheric Pressure Plasma Jet Driven by Tailored Voltage Waveforms," *Plasma Sources Science and Technology*, vol. 33, no. 7, 2024. [CrossRef] [Google Scholar] [Publisher Link]

[17] A. Sobota, O. Guaitella, and A. Rousseau, "The Influence of the Geometry and Electrical Characteristics on the Formation of the Atmospheric Pressure Plasma Jet," *Plasma Sources Science and Technology*, vol. 23, no. 2, 2014. [CrossRef] [Google Scholar] [Publisher Link]

[18] Han Xu et al., "Comparison between the Water Activation Effects by Pulsed and Sinusoidal Helium Plasma Jets," *Physics of Plasmas*, vol. 25, 2018. [CrossRef] [Google Scholar] [Publisher Link]

[19] Giichiro Uchida, Kosuke Takenaka, and Yuichi Setsuhara, "Effects of Discharge Voltage Waveform on the Discharge Characteristics in a Helium Atmospheric Plasma Jet," *Journal of Applied Physics*, vol. 117, 2015. [CrossRef] [Google Scholar] [Publisher Link]

[20] Shanti K. Thagunna, Vladimir I. Kolobov, and Gary P. Zank, "Self-Pulsing of Dielectric Barrier Discharges at Low Driving Frequencies," *Physics of Plasmas*, vol. 31, 2024. [CrossRef] [Google Scholar] [Publisher Link]

[21] Abdulrahman H. Basher, and Abdel-Aleam H. Mohamed, "Laminar and Turbulent Flow Modes of Cold Atmospheric Pressure Argon Plasma Jet," *Journal of Applied Physics*, vol. 123, 2018. [CrossRef] [Google Scholar] [Publisher Link]

[22] David E. Ashpis, Matthew C. Laun, and Elmer L. Griebeler, "Progress Toward Accurate Measurements of Power Consumptions of DBD Plasma Actuators," *50th AIAA Aerospace Sciences Meeting includinmg the New Horizons Forum and Aerospace Exposition*, Nashville, Tennessee, 2012. [CrossRef] [Google Scholar] [Publisher Link]